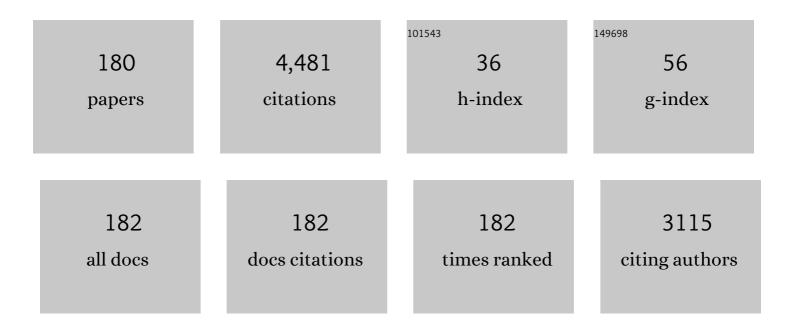
Tsuyoshi Murase

List of Publications by Year in descending order

Source: https://exaly.com/author-pdf/300648/publications.pdf Version: 2024-02-01



Τειινοςμι Μιιρλεγ

#	Article	IF	CITATIONS
1	Three-Dimensional Corrective Osteotomy of Malunited Fractures of the Upper Extremity with Use of a Computer Simulation System. Journal of Bone and Joint Surgery - Series A, 2008, 90, 2375-2389.	3.0	207
2	Interconnected porous hydroxyapatite ceramics for bone tissue engineering. Journal of the Royal Society Interface, 2009, 6, S341-8.	3.4	163
3	Interosseous Membrane of the Forearm: An Anatomical Study of Ligament Attachment Locations. Journal of Hand Surgery, 2009, 34, 415-422.	1.6	163
4	Methylcobalamin increases Erk1/2 and Akt activities through the methylation cycle and promotes nerve regeneration in a rat sciatic nerve injury model. Experimental Neurology, 2010, 222, 191-203.	4.1	130
5	In vivo elbow biomechanical analysis during flexion: three-dimensional motion analysis using magnetic resonance imaging. Journal of Shoulder and Elbow Surgery, 2004, 13, 441-447.	2.6	99
6	Distal Radius Osteotomy with Volar Locking Plates Based on Computer Simulation. Clinical Orthopaedics and Related Research, 2011, 469, 1766-1773.	1.5	95
7	Interosseous Membrane of the Forearm: Length Change of Ligaments During Forearm Rotation. Journal of Hand Surgery, 2009, 34, 685-691.	1.6	91
8	Computer-Assisted Corrective Osteotomy for Malunited Diaphyseal Forearm Fractures. Journal of Bone and Joint Surgery - Series A, 2012, 94, e150.	3.0	89
9	Capitate-based kinematics of the midcarpal joint during wrist radioulnar deviation: an in vivo three-dimensional motion analysis. Journal of Hand Surgery, 2004, 29, 668-675.	1.6	86
10	Accuracy analysis of threeâ€dimensional bone surface models of the forearm constructed from multidetector computed tomography data. International Journal of Medical Robotics and Computer Assisted Surgery, 2009, 5, 452-457.	2.3	85
11	Preoperative, Computer Simulation-Based, Three-Dimensional Corrective Osteotomy for Cubitus Varus Deformity with Use of a Custom-Designed Surgical Device. Journal of Bone and Joint Surgery - Series A, 2013, 95, e173.	3.0	78
12	In Vivo Three-Dimensional Kinematics of the Midcarpal Joint of the Wrist. Journal of Bone and Joint Surgery - Series A, 2006, 88, 611.	3.0	74
13	Open Repair of Foveal Avulsion of the Triangular Fibrocartilage Complex and Comparison by Types of Injury Mechanism. Journal of Hand Surgery, 2010, 35, 1955-1963.	1.6	74
14	In vivo three-dimensional wrist motion analysis using magnetic resonance imaging and volume-based registration. Journal of Orthopaedic Research, 2005, 23, 750-756.	2.3	69
15	Corrective Osteotomy for Malunited Intra-Articular Fracture of the Distal Radius Using a Custom-Made Surgical Guide Based on Three-Dimensional Computer Simulation: Case Report. Journal of Hand Surgery, 2008, 33, 835-840.	1.6	69
16	Change in the Length of the Ulnocarpal Ligaments During Radiocarpal Motion: Possible Impact on Triangular Fibrocartilage Complex Foveal Tears. Journal of Hand Surgery, 2008, 33, 1278-1286.	1.6	69
17	Relationship Between the Fracture Location and the Kinematic Pattern in Scaphoid Nonunion. Journal of Hand Surgery, 2008, 33, 1459-1468.	1.6	68
18	Electrospun nanofiber sheets incorporating methylcobalamin promote nerve regeneration and functional recovery in a rat sciatic nerve crush injury model. Acta Biomaterialia, 2017, 53, 250-259.	8.3	68

#	Article	IF	CITATIONS
19	Three-dimensional analysis of cubitus varus deformity after supracondylar fractures of the humerus. Journal of Shoulder and Elbow Surgery, 2011, 20, 440-448.	2.6	60
20	Interleukin-1 beta promotes sensory nerve regeneration after sciatic nerve injury. Neuroscience Letters, 2008, 440, 130-133.	2.1	58
21	Patterns of Carpal Deformity in Scaphoid Nonunion: A 3-Dimensional and Quantitative Analysis. Journal of Hand Surgery, 2005, 30, 1136-1144.	1.6	53
22	3-Dimensional Prebent Plate Fixation in Corrective Osteotomy of Malunited Upper Extremity Fractures Using a Real-Sized Plastic Bone Model Prepared by Preoperative Computer Simulation. Journal of Hand Surgery, 2013, 38, 909-919.	1.6	53
23	Derotational osteotomy at the shafts of the radius and ulna for congenital radioulnar synostosis. Journal of Hand Surgery, 2003, 28, 133-137.	1.6	52
24	The Triquetrum-Hamate joint: an anatomic and in vivo three-dimensional kinematic study. Journal of Hand Surgery, 2003, 28, 797-805.	1.6	51
25	Anterior Wedge-Shaped Bone Graft for Old Scaphoid Fractures or Non-Unions. Journal of Hand Surgery, 1995, 20, 194-200.	0.8	50
26	Accuracy of corrective osteotomy using a custom-designed device based on a novel computer simulation system. Journal of Orthopaedic Science, 2011, 16, 85-92.	1.1	48
27	Postoperative accuracy analysis of three-dimensional corrective osteotomy for cubitus varus deformity with a custom-made surgical guide based on computer simulation. Journal of Shoulder and Elbow Surgery, 2015, 24, 242-249.	2.6	46
28	IL-1β promotes neurite outgrowth by deactivating RhoA via p38 MAPK pathway. Biochemical and Biophysical Research Communications, 2008, 365, 375-380.	2.1	44
29	Threeâ€dimensional corrective osteotomy using a patientâ€specific osteotomy guide and bone plate based on a computer simulation system: accuracy analysis in a cadaver study. International Journal of Medical Robotics and Computer Assisted Surgery, 2014, 10, 196-202.	2.3	44
30	The in Vivo Isometric Point of the Lateral Ligament of the Elbow. Journal of Bone and Joint Surgery - Series A, 2007, 89, 2011-2017.	3.0	42
31	Long-Term Results of Surgery for Forearm Deformities in Patients with Multiple Cartilaginous Exostoses. Journal of Bone and Joint Surgery - Series A, 2007, 89, 1993-1999.	3.0	41
32	Corrective osteotomy using customized hydroxyapatite implants prepared by preoperative computer simulation. International Journal of Medical Robotics and Computer Assisted Surgery, 2010, 6, 186-193.	2.3	40
33	Methylcobalamin promotes the differentiation of Schwann cells and remyelination in lysophosphatidylcholine-induced demyelination of the rat sciatic nerve. Frontiers in Cellular Neuroscience, 2015, 9, 298.	3.7	39
34	Kinematics of the Thoracic Spine in Trunk Rotation. Spine, 2012, 37, E1318-E1328.	2.0	38
35	The in Vivo Isometric Point of the Lateral Ligament of the Elbow. Journal of Bone and Joint Surgery - Series A, 2007, 89, 2011-2017.	3.0	38
36	Modulation of peritendinous adhesion formation by alginate solution in a rabbit flexor tendon model. Journal of Biomedical Materials Research - Part B Applied Biomaterials, 2007, 80B, 273-279.	3.4	37

#	Article	IF	CITATIONS
37	Morphologic Evaluation of Chronic Radial Head Dislocation: Three-dimensional and Quantitative Analyses. Clinical Orthopaedics and Related Research, 2010, 468, 2410-2418.	1.5	36
38	Operative Technique of a New Decompression Procedure for Kienböck Disease: Partial Capitate Shortening. Techniques in Hand and Upper Extremity Surgery, 2004, 8, 110-115.	0.6	35
39	Patterns of bone defect in scaphoid nonunion: A 3-dimensional and quantitative analysis. Journal of Hand Surgery, 2005, 30, 359-365.	1.6	34
40	Morphometric Analysis of the Femur in Cerebral Palsy. Journal of Pediatric Orthopaedics, 2010, 30, 568-574.	1.2	34
41	Does Three-dimensional Computer Simulation Improve Results of Scaphoid Nonunion Surgery?. Clinical Orthopaedics and Related Research, 2005, &NA, 143-150.	1.5	33
42	In vivo three-dimensional motion analysis of the forearm with radioulnar synostosis treated by the kanaya procedure. Journal of Orthopaedic Research, 2006, 24, 1028-1035.	2.3	33
43	Sacroiliac joint motion in patients with degenerative lumbar spine disorders. Journal of Neurosurgery: Spine, 2015, 23, 209-216.	1.7	33
44	Akt/mammalian target of rapamycin signaling pathway regulates neurite outgrowth in cerebellar granule neurons stimulated by methylcobalamin. Neuroscience Letters, 2011, 495, 201-204.	2.1	32
45	Comparison of three dimensional and radiographic measurements in the analysis of distal radius malunion. Journal of Hand Surgery: European Volume, 2013, 38, 133-143.	1.0	32
46	Tailorâ€made surgical guide based on rapid prototyping technique for cup insertion in total hip arthroplasty. International Journal of Medical Robotics and Computer Assisted Surgery, 2009, 5, 164-169.	2.3	31
47	Kinematics of the thoracic spine in trunk lateral bending: inÂvivo three-dimensional analysis. Spine Journal, 2014, 14, 1991-1999.	1.3	31
48	InÂvivo and 3-dimensional functional anatomy of the anterior bundle of the medial collateral ligament of the elbow. Journal of Shoulder and Elbow Surgery, 2012, 21, 1006-1012.	2.6	29
49	Three-dimensional suitability assessment of three types of osteochondral autograft for ulnar coronoid process reconstruction. Journal of Shoulder and Elbow Surgery, 2014, 23, 143-150.	2.6	29
50	Cylindrical Corrective Osteotomy for Madelung Deformity Using a Computer Simulation: Case Report. Journal of Hand Surgery, 2013, 38, 1925-1932.	1.6	28
51	THE DORSAL CUTANEOUS BRANCH OF THE ULNAR NERVE: AN ANATOMICAL STUDY. Hand Surgery, 2010, 15, 165-168.	0.6	27
52	Three-dimensional deformity analysis of malunited distal radius fractures and their influence on wrist and forearm motion. Journal of Hand Surgery: European Volume, 2012, 37, 506-512.	1.0	27
53	Corrective osteotomy for malunited both bones fractures of the forearm with radial head dislocations using a custom-made surgical guide: two case reports. Journal of Shoulder and Elbow Surgery, 2012, 21, e1-e8.	2.6	27
54	Three-Dimensional Analysis of Acromial Morphologic Characteristics in Patients With and Without Rotator Cuff Tears Using a Reconstructed Computed Tomography Model. American Journal of Sports Medicine, 2014, 42, 2621-2626.	4.2	26

#	Article	IF	CITATIONS
55	Altered bone density and stress distribution patterns in long-standing cubitus varus deformity and their effect during early osteoarthritis of the elbow. Osteoarthritis and Cartilage, 2018, 26, 72-83.	1.3	26
56	Three-Dimensional Corrective Osteotomy for Malunited Fractures of the Upper Extremity Using Patient-Matched Instruments. Journal of Bone and Joint Surgery - Series A, 2019, 101, 710-721.	3.0	26
57	Does cubitus varus cause morphologic and alignment changes in the elbow joint?. Journal of Shoulder and Elbow Surgery, 2013, 22, 915-923.	2.6	25
58	The association between cubital tunnel morphology and ulnar neuropathy in patients with elbow osteoarthritis. Journal of Shoulder and Elbow Surgery, 2014, 23, 938-945.	2.6	25
59	Changes in Shape and Length of the Collateral and Accessory Collateral Ligaments of the Metacarpophalangeal Joint During Flexion. Journal of Bone and Joint Surgery - Series A, 2011, 93, 1318-1325.	3.0	24
60	Three-dimensional analysis of acute plastic bowing deformity of ulna in radial head dislocation or radial shaft fracture using a computerized simulation system. Journal of Shoulder and Elbow Surgery, 2012, 21, 1644-1650.	2.6	24
61	Arthroscopic debridement in the treatment of patients with osteoarthritis of the elbow, based on computer simulation. Bone and Joint Journal, 2014, 96-B, 237-241.	4.4	24
62	Intra-articular distal ulnar fractures associated with distal radial fractures in older adults: early experience in fixation of the radius and leaving the ulna unfixed. Journal of Hand Surgery: European Volume, 2009, 34, 592-597.	1.0	22
63	Morphometric Analysis of Acetabular Dysplasia in Cerebral Palsy: Three-dimensional CT Study. Journal of Pediatric Orthopaedics, 2009, 29, 896-902.	1.2	22
64	In Vivo 3-Dimensional Analysis of Dorsal Intercalated Segment Instability Deformity Secondary to Scapholunate Dissociation: A Preliminary Report. Journal of Hand Surgery, 2013, 38, 1346-1355.	1.6	22
65	Volar morphology of the distal radius in axial planes: A quantitative analysis. Journal of Orthopaedic Research, 2015, 33, 496-503.	2.3	22
66	Three-Dimensional Kinematics of the Rheumatoid Wrist After Partial Arthrodesis. Journal of Bone and Joint Surgery - Series A, 2009, 91, 2180-2187.	3.0	21
67	Validation of the femoral component placement during hip resurfacing: a comparison between the conventional jig, patientâ€specific template, and CTâ€based navigation. International Journal of Medical Robotics and Computer Assisted Surgery, 2013, 9, 223-229.	2.3	21
68	In vivo three-dimensional motion analysis of osteoarthritic knees. Modern Rheumatology, 2013, 23, 646-652.	1.8	21
69	InÂvivo three-dimensional elbow biomechanics during forearm rotation. Journal of Shoulder and Elbow Surgery, 2016, 25, 112-119.	2.6	21
70	Three-dimensional distribution of articular cartilage thickness in the elderly cadaveric acetabulum: a new method using three-dimensional digitizer and CT. Osteoarthritis and Cartilage, 2010, 18, 795-802.	1.3	20
71	3-Dimensional Deformity Analysis of Malunited Forearm Diaphyseal Fractures. Journal of Hand Surgery, 2013, 38, 1356-1365.	1.6	20
72	Morphological evaluation of the distal interosseous membrane using ultrasound. European Journal of Orthopaedic Surgery and Traumatology, 2014, 24, 1095-1100.	1.4	20

#	Article	IF	CITATIONS
73	Neurotropin attenuates local inflammatory response and inhibits demyelination induced by chronic constriction injury of the mouse sciatic nerve. Biologicals, 2016, 44, 206-211.	1.4	19
74	Utility of Distal Forearm DXA as a Screening Tool for Primary Osteoporotic Fragility Fractures of the Distal Radius. JBJS Open Access, 2020, 5, e0036.	1.5	19
75	Extensor Tendon Rupture due to Kienböck's Disease. Journal of Hand Surgery, 1997, 22, 597-598.	0.8	18
76	Correction of severe wrist deformity following physeal arrest of the distal radius with the aid of a three-dimensional computer simulation. Archives of Orthopaedic and Trauma Surgery, 2009, 129, 1465-1471.	2.4	18
77	In Vivo Three-dimensional Motion Analysis of Chronic Radial Head Dislocations. Clinical Orthopaedics and Related Research, 2012, 470, 2746-2755.	1.5	18
78	InÂVivo 3-Dimensional Kinematics of Thumb Carpometacarpal Joint During Thumb Opposition. Journal of Hand Surgery, 2018, 43, 182.e1-182.e7.	1.6	18
79	2D–3D reconstruction of distal forearm bone from actual X-ray images of the wrist using convolutional neural networks. Scientific Reports, 2021, 11, 15249.	3.3	18
80	Effects of Weekly Teriparatide Administration for Vertebral Stability and Bony Union in Patients with Acute Osteoporotic Vertebral Fractures. Asian Spine Journal, 2019, 13, 763-771.	2.0	18
81	Design of super-elastic biodegradable scaffolds with longitudinally oriented microchannels and optimization of the channel size for Schwann cell migration. Science and Technology of Advanced Materials, 2012, 13, 064207.	6.1	17
82	Neurotropin® Accelerates the Differentiation of Schwann Cells and Remyelination in a Rat Lysophosphatidylcholine-Induced Demyelination Model. International Journal of Molecular Sciences, 2018, 19, 516.	4.1	17
83	In vivo three-dimensional kinematics of total elbow arthroplasty using fluoroscopic imaging. International Orthopaedics, 2010, 34, 847-854.	1.9	16
84	Open Reduction and 3-Dimensional Ulnar Osteotomy for Chronic Radial Head Dislocation Using a Computer-Generated Template: Case Report. Journal of Hand Surgery, 2012, 37, 517-522.	1.6	16
85	A comparison of 3-D computed tomography versus 2-D radiography measurements of ulnar variance and ulnolunate distance during forearm rotation. Journal of Hand Surgery: European Volume, 2014, 39, 526-532.	1.0	16
86	Validation of patient specific surgical guides in total hip arthroplasty. International Journal of Medical Robotics and Computer Assisted Surgery, 2014, 10, 113-120.	2.3	16
87	Radiographic study of joint destruction patterns in the rheumatoid elbow. Clinical Rheumatology, 2007, 26, 515-519.	2.2	15
88	Ulnar Variance: Its Relationship to Ulnar Foveal Morphology and Forearm Kinematics. Journal of Hand Surgery, 2012, 37, 729-735.	1.6	15
89	Impact of Distal Ulnar Fracture Malunion on Distal Radioulnar Joint Instability: A Biomechanical Study of the Distal Interosseous Membrane Using a Cadaver Model. Journal of Hand Surgery, 2017, 42, e185-e191.	1.6	15
90	Three-dimensional analysis of deformities of the radius and ulna in congenital proximal radioulnar synostosis. Journal of Hand Surgery: European Volume, 2018, 43, 739-743.	1.0	15

#	Article	IF	CITATIONS
91	Combination of Electrospun Nanofiber Sheet Incorporating Methylcobalamin and PGA-Collagen Tube for Treatment of a Sciatic Nerve Defect in a Rat Model. Journal of Bone and Joint Surgery - Series A, 2020, 102, 245-253.	3.0	15
92	Kinematic Changes in Elbow Osteoarthritis: In Vivo and 3-Dimensional Analysis Using Computed Tomographic Data. Journal of Hand Surgery, 2013, 38, 957-964.	1.6	14
93	In Vivo Three-Dimensional Analysis of Malunited Forearm Diaphyseal Fractures with Forearm Rotational Restriction. Journal of Bone and Joint Surgery - Series A, 2018, 100, e113.	3.0	14
94	Pseudomallet finger associated with exostosis of the phalanx: A report of 2 cases. Journal of Hand Surgery, 2002, 27, 817-820.	1.6	13
95	USE OF THE VOLAR FIXED ANGLE PLATE FOR COMMINUTED DISTAL RADIUS FRACTURES AND AUGMENTATION WITH A HYDROXYAPATITE BONE GRAFT SUBSTITUTE. Hand Surgery, 2011, 16, 29-37.	0.6	13
96	In vivo 3D kinematic changes in the cervical spine after laminoplasty for cervical spondylotic myelopathy. Journal of Neurosurgery: Spine, 2014, 21, 417-424.	1.7	13
97	Computer assisted planning and custom-made surgical guide for malunited pronation deformity after first metatarsophalangeal joint arthrodesis in rheumatoid arthritis: A case report. Computer Aided Surgery, 2014, 19, 13-19.	1.8	13
98	Administration of Oxygen Ultra-Fine Bubbles Improves Nerve Dysfunction in a Rat Sciatic Nerve Crush Injury Model. International Journal of Molecular Sciences, 2018, 19, 1395.	4.1	13
99	Calcific tendinitis at the biceps insertion causing rotatory limitation of the forearm: A case report. Journal of Hand Surgery, 1994, 19, 266-268.	1.6	12
100	Analysis of Radiocarpal and Midcarpal Motion in Stable and Unstable Rheumatoid Wrists Using 3-Dimensional Computed Tomography. Journal of Hand Surgery, 2008, 33, 189-197.	1.6	12
101	Methylcobalamin promotes proliferation and migration and inhibits apoptosis of C2C12 cells via the Erk1/2 signaling pathway. Biochemical and Biophysical Research Communications, 2014, 443, 871-875.	2.1	12
102	Open Wedge Osteotomy with Ulnar Shortening for Madelung Deformity Using a Computer-Generated Template. journal of hand surgery Asian-Pacific volume, The, 2017, 22, 538-543.	0.4	12
103	Surgical treatment of hand disorders in Farber's disease: A case report. Journal of Hand Surgery, 2002, 27, 503-507.	1.6	11
104	RUPTURE OF THE FLEXOR TENDON AFTER MALUNITED COLLES' FRACTURE. Scandinavian Journal of Plastic and Reconstructive Surgery and Hand Surgery, 2003, 37, 188-191.	0.6	11
105	A three-dimensional quantitative analysis of carpal deformity in rheumatoid wrists. Journal of Bone and Joint Surgery: British Volume, 2007, 89-B, 490-494.	3.4	11
106	Three-dimensional kinematics of the lunate, hamate, capitate and triquetrum with type 1 or 2 lunate morphology. Journal of Hand Surgery: European Volume, 2018, 43, 380-386.	1.0	11
107	Bone resorption of the greater tuberosity after open reduction and internal fixation of complex proximal humeral fractures: fragment characteristics and intraoperative risk factors. Journal of Shoulder and Elbow Surgery, 2021, 30, 1626-1635.	2.6	11
108	Three-dimensional motion of the uncovertebral joint during head rotation. Journal of Neurosurgery: Spine, 2012, 17, 327-333.	1.7	10

#	Article	IF	CITATIONS
109	Radiofrequency ablation for treatment for osteoid osteoma of the scapula using a new three-dimensional fluoroscopic navigation system. European Journal of Orthopaedic Surgery and Traumatology, 2014, 24, 231-235.	1.4	10
110	InÂVivo 3-Dimensional Analysis of Stage III Kienböck Disease: Pattern of Carpal Deformity and Radioscaphoid Joint Congruity. Journal of Hand Surgery, 2015, 40, 74-80.	1.6	10
111	InÂVivo Scaphoid Motion During Thumb and Forearm Motion in Casts for Scaphoid Fractures. Journal of Hand Surgery, 2017, 42, 475.e1-475.e7.	1.6	10
112	Validation of patientâ€specific surgical guides for femoral neck cutting in total hip arthroplasty through the anterolateral approach. International Journal of Medical Robotics and Computer Assisted Surgery, 2017, 13, e1830.	2.3	10
113	Rotational Corrective Osteotomy for Malunited Distal Diaphyseal Radius Fractures in Children and Adolescents. Journal of Hand Surgery, 2018, 43, 286.e1-286.e8.	1.6	10
114	In vivo 3D kinematics of the upper cervical spine during head rotation in rheumatoid arthritis. Journal of Neurosurgery: Spine, 2014, 20, 404-410.	1.7	9
115	Three-Dimensional Corrective Osteotomy for Cubitus Varus Deformity with Use of Custom-Made Surgical Guides. JBJS Essential Surgical Techniques, 2014, 4, e6.	0.8	9
116	Three-dimensional inÂvivo kinematics during elbow flexion in patients with lateral humeral condyle nonunion by an image-matching technique. Journal of Shoulder and Elbow Surgery, 2014, 23, 318-326.	2.6	9
117	Three-dimensional analysis of osteophyte formation on distal radius following scaphoid nonunion. Journal of Orthopaedic Science, 2017, 22, 50-55.	1.1	9
118	A comparison of corrective osteotomies using dorsal and volar fixation for malunited distal radius fractures. International Orthopaedics, 2018, 42, 2873-2879.	1.9	9
119	Regional Distribution of Articular Cartilage Thickness in the Elbow Joint. JBJS Open Access, 2019, 4, e0011.	1.5	9
120	InÂvivo three-dimensional motion analysis of osteoarthritic knees. Modern Rheumatology, 2013, 23, 646-652.	1.8	9
121	MASSIVE VASCULAR LEIOMYOMA OF THE HAND. Scandinavian Journal of Plastic and Reconstructive Surgery and Hand Surgery, 2003, 37, 125-127.	0.6	8
122	Changes in length of the radioulnar ligament and distal oblique bundle after Colles' fracture. Journal of Plastic Surgery and Hand Surgery, 2013, 47, 409-414.	0.8	8
123	Surgical Technique of Corrective Osteotomy for Malunited Distal Radius Fracture Using the Computer-Simulated Patient Matched Instrument. journal of hand surgery Asian-Pacific volume, The, 2016, 21, 133-139.	0.4	8
124	Enchondromatosis-associated oligodendroglioma: case report and literature review. Brain Tumor Pathology, 2018, 35, 36-40.	1.7	8
125	Validation of the registration accuracy of navigation-assisted arthroscopic débridement for elbow osteoarthritis. Journal of Shoulder and Elbow Surgery, 2019, 28, 2400-2408.	2.6	8
126	Artificial intelligence to diagnosis distal radius fracture using biplane plain X-rays. Journal of Orthopaedic Surgery and Research, 2021, 16, 694.	2.3	8

#	Article	IF	CITATIONS
127	A histochemical study of the biceps brachii muscle cross-innervated by intercostal nerves:6 cases of brachial plexus injuries operated with nerve-crossing. Acta Orthopaedica, 1994, 65, 204-206.	1.4	7
128	Morphologic analysis of the medullary canal in rheumatoid elbows. Journal of Shoulder and Elbow Surgery, 2009, 18, 33-37.	2.6	7
129	Three-Dimensional Corrective Osteotomy for Malunited Diaphyseal Forearm Fractures Using Custom-Made Surgical Guides Based on Computer Simulation. JBJS Essential Surgical Techniques, 2012, 2, e24.	0.8	7
130	3D morphometric analysis of laminae and facet joints in patients with degenerative spondylolisthesis. Modern Rheumatology, 2015, 25, 756-760.	1.8	7
131	Cartilage wear patterns in severe osteoarthritis of the trapeziometacarpal joint: a quantitative analysis. Osteoarthritis and Cartilage, 2019, 27, 1152-1162.	1.3	7
132	Single-plane rotational osteotomy for cubitus varus deformity based on preoperative computer simulation. Journal of Orthopaedic Science, 2019, 24, 945-951.	1.1	7
133	Three-dimensional analysis of displacement characteristics of dorsally angulated intra-articular distal radial fractures. Journal of Hand Surgery: European Volume, 2020, 45, 339-347.	1.0	7
134	Palmar Dislocation of the Metacarpophalangeal Joint of the Finger. Journal of Hand Surgery, 2004, 29, 90-93.	0.8	6
135	Tumorous Calcification Causing Carpal Tunnel Syndrome. Handchirurgie Mikrochirurgie Plastische Chirurgie, 2008, 40, 294-298.	0.3	6
136	Radiographic study on the pattern of wrist joint destruction in rheumatoid arthritis. Clinical Rheumatology, 2011, 30, 353-359.	2.2	6
137	SYNOVIAL CHONDROMATOSIS OF THE METACARPOPHALANGEAL JOINT: A CASE REPORT AND LITERATURE REVIEW. Hand Surgery, 2012, 17, 395-398.	0.6	6
138	Corticoplasty for Improved Appearance of Hands With Ollier Disease. Journal of Hand Surgery, 2012, 37, 2294-2299.	1.6	6
139	Corrective Osteotomy and Ligament Repair for Longstanding Radial Collateral Ligament Tear of the Proximal Interphalangeal Joint: Case Series. Journal of Hand Surgery, 2012, 37, 440-445.	1.6	6
140	In-vivo biomechanical analysis of osteochondritis dissecans of the humeral trochlea. Journal of Pediatric Orthopaedics Part B, 2013, 22, 392-396.	0.6	6
141	Corrective osteotomy assisted by computer simulation for a malunited intra-articular fracture of the distal humerus: two case reports. Archives of Orthopaedic and Trauma Surgery, 2016, 136, 1499-1505.	2.4	6
142	Physeal bar resection using a patient-specific guide with intramedullary endoscopic assistance for partial physeal arrest of the distal radius. Archives of Orthopaedic and Trauma Surgery, 2018, 138, 1179-1188.	2.4	6
143	Analysis of forearm rotational motion using biplane fluoroscopic intensity-based 2D–3D matching. Journal of Biomechanics, 2019, 89, 128-133.	2.1	6
144	Quantitative Analysis for the Change in Lengths of the Radius and Ulna in Missed Bado Type I Monteggia Fracture. Journal of Pediatric Orthopaedics, 2020, 40, e922-e926.	1.2	6

#	Article	IF	CITATIONS
145	Three-dimensional evaluations of preoperative planning reproducibility for the osteosynthesis of distal radius fractures. Journal of Orthopaedic Surgery and Research, 2021, 16, 131.	2.3	6
146	IN VIVO THREE-DIMENSIONAL KINEMATICS OF THE MIDCARPAL JOINT OF THE WRIST. Journal of Bone and Joint Surgery - Series A, 2006, 88, 611-621.	3.0	6
147	Computer-aided parachute guiding system for closed reduction of diaphyseal fractures. International Journal of Medical Robotics and Computer Assisted Surgery, 2014, 10, 325-331.	2.3	5
148	Use of a Custom-made Surgical Guide in Total Ankle Arthroplasty in Rheumatoid Arthritis Cases. Techniques in Orthopaedics, 2014, 29, 103-112.	0.2	5
149	Median nerve neuropathy in the forearm due to recurrence of anterior wrist ganglion that originates from the scaphotrapezial joint: Case Report. Journal of Brachial Plexus and Peripheral Nerve Injury, 2014, 07, e22-e25.	1.0	5
150	Prediction of forearm bone shape based on partial least squares regression from partial shape. International Journal of Medical Robotics and Computer Assisted Surgery, 2017, 13, e1807.	2.3	5
151	Three-dimensional scapular dyskinesis in hook-plated acromioclavicular dislocation including hook motion. Journal of Shoulder and Elbow Surgery, 2018, 27, 1117-1124.	2.6	5
152	Threeâ€Ðimensional In Vivo Analysis of Malunited Distal Radius Fractures With Restricted Forearm Rotation. Journal of Orthopaedic Research, 2019, 37, 1881-1891.	2.3	5
153	Bone density measurements from CT scans may predict the healing capacity of scaphoid waist fractures. Bone and Joint Journal, 2020, 102-B, 1200-1209.	4.4	5
154	Treatment of juxta-articular intraosseous cystic lesions in rheumatoid arthritis patients with interconnected porous calcium hydroxyapatite ceramic. Modern Rheumatology, 2009, 19, 180-186.	1.8	5
155	Corrective osteotomy for hyperextended elbow with limited flexion due to supracondylar fracture malunion. Journal of Shoulder and Elbow Surgery, 2018, 27, 1357-1365.	2.6	4
156	Degenerative changes in the elbow joint after radial head excision for fracture: quantitative 3-dimensional analysis of bone density, stress distribution, and bone morphology. Journal of Shoulder and Elbow Surgery, 2021, 30, e199-e211.	2.6	4
157	Attritional rupture of the extensor pollicis longus tendon by an osseous spur more than 30 years after wrist injury: A case report. Journal of Plastic Surgery and Hand Surgery, 2014, 48, 452-454.	0.8	3
158	A Nanofiber Sheet Incorporating Vitamin B12 Promotes Nerve Regeneration in a Rat Neurorrhaphy Model. Plastic and Reconstructive Surgery - Global Open, 2019, 7, e2538.	0.6	3
159	In vivo three-dimensional scapular kinematic alterations after reverse total shoulder arthroplasty. Journal of Orthopaedic Surgery, 2020, 28, 230949902092197.	1.0	3
160	Computer-Aided Assessment of Displacement and Reduction of Distal Radius Fractures. Diagnostics, 2021, 11, 719.	2.6	3
161	Utility of a 3-dimensionally printed color-coded bone model to visualize impinging osteophytes for arthroscopic débridement arthroplasty in elbow osteoarthritis. Journal of Shoulder and Elbow Surgery, 2021, 30, 1152-1158.	2.6	3
162	Arthroscopic Debridement of Elbow Osteoarthritis Using CT-Based Computer-Aided Navigation Systems Is Accurate. Arthroscopy, Sports Medicine, and Rehabilitation, 2021, 3, e1687-e1696.	1.7	3

#	Article	IF	CITATIONS
163	In Vivo Analysis of Three-Dimensional Dynamic Scapular Dyskinesis in Scapular or Clavicular Fractures. Acta Medica Okayama, 2017, 71, 151-159.	0.2	3
164	Rotational and Varus Instability in Chronic Lateral Ankle Instability: In Vivo 3D Biomechanical Analysis. Acta Medica Okayama, 2018, 72, 583-589.	0.2	3
165	Carpal-tunnel syndrome in hemodialysis: Syndrome diagnosed in 8 of 60 patients. Acta Orthopaedica, 1993, 64, 475-478.	1.4	2
166	Giant aneurysm of the ulnar artery in the palm treated by resection and microvascular reconstruction. Scandinavian Journal of Plastic and Reconstructive Surgery and Hand Surgery, 2009, 43, 113-116.	0.6	2
167	3D corrective osteotomy of malunited upper limb fractures. BMC Proceedings, 2015, 9, .	1.6	2
168	Morphology and kinematics studies of the upper extremity and its clinical application in deformity correction. Journal of Orthopaedic Science, 2018, 23, 722-733.	1.1	2
169	Intra-articular corrective osteotomy for intra-articular malunion of distal radius fracture using three-dimensional surgical computer simulation and patient-matched instrument. Journal of Orthopaedic Science, 2020, 25, 847-853.	1.1	2
170	Comparison of the Orientation Angles of Volar Locking Plate Distal Ulnar Locking Screw for Distal Radius Fractures. Journal of Hand Surgery, 2021, , .	1.6	2
171	Comparing the locking screw direction of three locking plates for lateral clavicle fractures: a simulation study. BMC Musculoskeletal Disorders, 2021, 22, 812.	1.9	2
172	DEVIATION OF A FINGER AT THE PROXIMAL INTERPHALANGEAL JOINT CAUSED BY JUXTA-ARTICULAR EXOSTOSIS. Scandinavian Journal of Plastic and Reconstructive Surgery and Hand Surgery, 2003, 37, 248-251.	0.6	1
173	Free flap transfer for complex regional pain syndrome type II. Case Reports in Plastic Surgery & Hand Surgery, 2014, 1, 1-4.	0.3	1
174	Combination of an Electrospun Nanofiber Sheet Incorporating Methylcobalamin and a PGA-Collagen Tube Promotes Nerve Regeneration and Functional Recovery in a Rat Sciatic Nerve Defect Model. Journal of Hand Surgery, 2018, 43, S32-S33.	1.6	1
175	The morphologicÂchange of the elbow with flexion contracture in upper obstetric brachial plexus palsy. Journal of Shoulder and Elbow Surgery, 2019, 28, 1764-1770.	2.6	1
176	In vivo 3-dimensional Kinematics of Cubitus Valgus after Non-united Lateral Humeral Condyle Fracture. Clinics in Shoulder and Elbow, 2018, 21, 151-157.	2.0	1
177	Spontaneous divergent elbow dislocation after Sauve-Kapandji procedure. Clinical Orthopaedics and Related Research, 2003, , 97-102.	1.5	1
178	A Quantitative Analysis of Subchondral Bone Density Around Osteochondritis Dissecans Lesions of the Capitellum. Journal of Hand Surgery, 2022, 47, 790.e1-790.e11.	1.6	0
179	Computer Simulation Surgery for Deformity Correction of the Upper Extremity. , 2016, , 271-291.		0
180	Lymphangioma of the Upper Extremity. Journal of Pediatric Orthopaedics, 1992, 12, 100-105.	1.2	0

11